IEEE Access
Multidisciplinary ⋮ Rapid Review ⋮ Open Access Journal

Received 11 April 2024, accepted 14 May 2024, date of publication 17 May 2024, date of current version 24 May 2024.

Digital Object Identifier 10.1109/ACCESS.2024.3402359

RESEARCH ARTICLE

Real-Time PVC Recognition System Design Based on Multi-Parameter SE-ResNet

DUAN LI[1], PEISEN LIU[1], TINGTING SUN[1], LIANXIANG LI[1], AND YIBAI XUE[2]
[1]School of Electronic Information Engineering, Zhengzhou University of Light Industry, Zhengzhou 450002, China
[2]Department of Cardiothoracic Surgery, The Fifth Affiliated Hospital of Zhengzhou University, Zhengzhou 450002, China

Corresponding author: Duan Li (liduan@hpu.edu.cn)

This work was supported in part by the National Natural Science Foundation of China under Grant 62106233, and in part by the Key Science and Technology Program of Henan Province under Grant 232102211003 and Grant 232102210017.

ABSTRACT The real-time and accurate detection of premature ventricular contractions (PVC) in patients is of great significance for preventing the occurrence of high-risk events such as sudden cardiac death and guiding cardiac surgical procedures such as radiofrequency ablation. To improve the diagnostic accuracy and real-time performance, and expand application scenarios, an economical wearable PVC real-time auxiliary diagnosis system based on the multi-parameter squeeze excitation residual network (MP-SE-ResNet) is proposed. We have realized the real-time acquisition, processing, and wireless transmission of dynamic ECGs based on ESP32, furthermore, realized the PVCs recognition based on MP-SE-ResNet. Using the lead-II ECGs in the MIT-BIH arrhythmia databases as training samples, and the network was evaluated using the remainder of this dataset and data recorded by our device, respectively. The accuracy of the MIT-BIH dataset reached 99.34%, and the sensitivity and specificity of PVC recognition reached 98.26% and 99.64%, respectively. Using the ECGs recorded by our system, we achieved the following results: the accuracy was 94.07%, the sensitivity and specificity of PVC were 92.76% and 97.63%, respectively. The experimental results show that the system meets the requirements of remote monitoring and auxiliary diagnosis. Therefore, it provides a new method and design idea for wearable remote arrhythmia monitoring and auxiliary diagnosis.

INDEX TERMS Wearable ECG device, ESP32, ECG cloud platform, multi-parameter SE-ResNet.

I. INTRODUCTION

Among patients with cardiovascular diseases, more than 80% of cardiovascular patients are combined with arrhythmias, which are highly likely to lead to malignant events such as stroke and sudden cardiac death [1], [2], [3]. Ventricular premature beat (PVC) is the most common reason of abnormal heartbeat [4]. Under the certain conditions, it can lead to life-threatening heart disease. Automatic detection of PVC based on wearable remote holter can effectively and timely prevent cardiac diseases such as arrhythmia and avoid the occurrence of malignant arrhythmia events. Real-time ECG monitoring of PVC can also accurately locate the occurrence time of ventricular premature beat and the location of premature beat source, so as to guide surgical procedures such as radio frequency ablation [5], [6], [7].

The associate editor coordinating the review of this manuscript and approving it for publication was Eyuphan Bulut.

However, the wearable devices are prone to introduce some problems such as interference and lead-fall, and massive real-time data and its individual and environmental variability put forward strict requirements on the implementation of pre-processing algorithms and arrhythmia accurate recognition [8], [9]. Therefore, the current wearable ECG arrhythmia diagnosis products are limited in terms of real-time functionality and application scenarios. For wearable ECG monitoring, technology challenges exist, and are mainly from the following two aspects. The first challenge comes from the physical implementation of the wearable smart ECG garment system, including textile sensor design [10], wearable client hardware circuit design for comfort measurement [11], [12], [13], [14]. The second comes from the big data processing, data storage, and long-term ECG cardiovascular diseases monitoring and deep-mining for specific arrhythmia type, which involves the efficient machine learning and improved deep learning methods [15], [16], [17], [18], [19], [20].

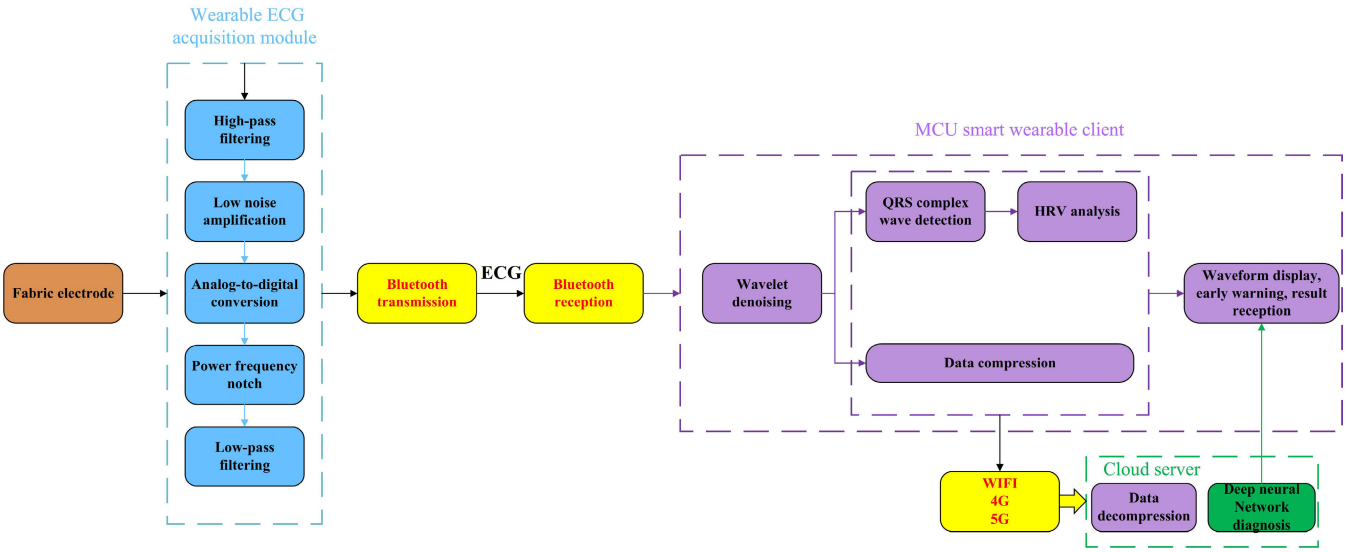

FIGURE 1. Overall design scheme.

Heart disease is sudden and progressive. This work intends to develop a wearable ECG analysis product which is suitable for multiple scenarios. The product uses the ESP32 as the client chip to perform ECG signal denoising, quality assessment, compression and data transmission, and receive arrhythmia diagnosis results from remote servers in time. Finally, the patients' heart health status would be analyzed in the cloud platform using multi-parameter squeeze-excitation ResNet (MP-SE-ResNet) model and malignant arrhythmia events can be detected in time. The key contributions of this work are:

- Proposed and designed the wearable ECG acquisition and processing system based on the BMD101 module and ESP32 microcontroller, which performs ECG signal acquisition, storage, processing, display, remote transmission, and reception.
- Proposed MP-SE-ResNet model for dynamic ECG PVC heartbeat recognition, which incorporates a feature recalculation strategy that enhances useful features and suppresses those irrelevant to the current task.
- Comparison of the proposed networks with existing state-of-the-art methods using the MIT-BIH arrhythmia database and the recorded data by our device.

The remainder of this paper is organized as follows. Section II is the related works. Section III described the system design scheme for this study. Section IV provides details of our software Working flow. In section V, we provide details of a MP-SE-ResNet based PVC recognition performance and the experimental results. A discussion is presented in Section VI. Finally, section VII concludes the paper.

II. RELATED WORKS

Continuously monitoring and recognition for life threating arrhythmia based on wearable and smartphone devices using deep-learning method become a hot topic in recent years [21], [22], [23]. As PVC often exhibits no obvious clinical symptoms during the attack and is a primary contributor to sudden cardiac death, there have been many research results on the real-time recognition of PVCs [24], [25], [26], [27]. Brito et al. [28] proposed a deep learning model based on ResNet architecture in 2019, achieving an accuracy of over 90% in experiments using the MIT-BIH arrhythmia database. In 2020, Li et al. [15] classified arrhythmias using a deep residual network, yielding a 99.38% classification accuracy on the MIT-BIH arrhythmia database. In 2021, Wang [29] proposed an enhanced gated recurrent unit network for PVC recognition, generating accuracies of 98.3% and 97.9% with the MIT-BIH arrhythmia database and China Physiological Signal Challenge 2018 database, respectively, using R-wave annotations provided by the databases. In 2022, Sarshar and Mirzaei [30] explored statistical features which include three morphological features (RS amplitude, QR amplitude, and QRS width) and seven statistical features are computed for each signal, and combined CNN model for PVC recognition on the MIT-BIH database, producing more effective diagnosis performance. In 2024, Ebrahimpoor et al. [31] proposed a Multi-Domain Feature Extraction and Auto-Encoder-based Feature Reduction method for PVC recognition, the algorithm is also evaluated using MIT-BIH database. But these studies did not outline a reliable way to classify and detect the accuracy of PVCs based on a wearable cardiac monitoring system in real-time.

In 2023, a PVC detection and classification system based on the Nexys 4 DDR FPGA board were proposed. Utilizing 4.36% of the total resources, they achieved an improved accuracy and sensitivity of 98.29% and 98.64% for PVC recognition, respectively [32]. Though FPGA has high computation speed, the power consumption and cost are higher compared with the general microcontroller.

TABLE 1. Advantages and disadvantages of the researches.

Researches	Advantages	Disadvantages
Brito et al. [28]	Proposed ResNet for arrhythmias	The accuracy is lower on MIT-BIH database, not using real-time wearable ECGs to evaluate the model
Li et al. [15]	The designed ResNet is robust and the accuracy for arrhythmias recognition is higher	Not using real-time wearable ECGs to evaluate the model
Jinbin Wang [29]	The first used enhanced gated recurrent unit network for PVC recognition	Not using real-time wearable ECGs to evaluate the proposed method
Sarshar et al. [30]	Using 10 ECG features fed to CNN for PVC recognition, higher efficient	The feature extraction capability of CNN cannot be fully utilized, not using real-time wearable ECGs to evaluation
Ebrahimpoor et al. [31]	New feature selection based on an Auto-Encoder	Not using real-time wearable ECGs to evaluate the proposed method
Gon et al.[32]	The PVC detection methods were performed on FPGA in real-time and achieved higher accuracy	The FPGA system is higher cost, not using real-time wearable ECGs to evaluate the algorithm

Though these methods perform well in PVC recognition, each of them has its advantages and disadvantages (as summarized in Table 1). Furthermore, the accuracy of many algorithms will diminish if the clinical dynamic wearable large ECG data is used [33], [34]. A study of 100 patients with atrial fibrillation revealed that 34% of wearable ECG recordings were algorithmically classified as ''unclassified'' due to unknown cause, baseline artifacts, or low amplitude recordings [35]. Therefore, the economic wearable smart ECG monitoring system design and the evolution of models or methods is crucial to enhance PVC detection performance, facilitating clinical applications.

III. SYSTEM DESIGN SCHEME

As shown in Figure 1, the system includes ECG signal acquisition, data transmission, primary control unit and remote deep-learning based monitoring and diagnosis cloud platform. The BMD101 ECG acquisition module was used to collect ECG data, and the data was sent to the main control unit through Bluetooth. The ESP32-WROOM-32 module was used to collect and process ECG signals, then upload them to the cloud server by the wifi embedded in the main control module based on the socket communication, and display real-time heart rate, HRV analysis, diagnosis results, etc. on the OLED display screen. The cloud platform aims to complete data reception, storage and real-time diagnosis. After receiving the signal sent by the main control, the cloud server stores the data in the user database, performs data analysis and subject-specific auxiliary diagnosis, and returns the diagnosis results to the main control unit.

A. ECG SIGNAL ACQUISITION MODULE

The stability and accuracy of ECG data acquisition directly affect the subsequent ECG data processing, heart rate calculation, ECG imaging and auxiliary diagnosis result, so the sensor is the key for the design of the heart detector [36], [37]. The signal acquisition module adopted in this design is the BMD101 ECG signal acquisition chip. The ECG acquisition module integrates SPP-C Bluetooth to collect ECG data and send the data packets to the main control. The module has low power consumption, 512Hz sampling rate, 16-bit AD conversion accuracy, and can use metal dry electrode or gel wet electrode to collect ECG signals with a frequency response of 0.5Hz∼100Hz. In order to meet the need of multi-scenario wearable applications, a modular method is adopted to integrate the BMD101 ECG signal acquisition chip, SPP-C Bluetooth module and power module into a PCB board, which can be easily embedded in the vest. Figure 2 shows the PCB circuit of ECG acquisition block and its usage method.

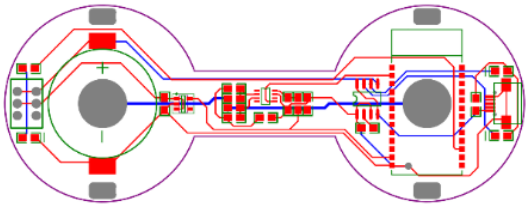

(a) PCB circuit of BMD101 ECG acquisition module

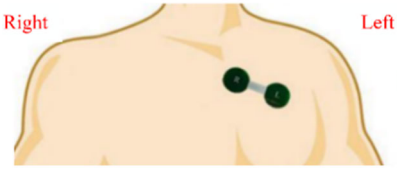

(b) Usage method

FIGURE 2. BMD101 acquisition module.

B. DESIGN OF MAIN CONTROL UNIT BASED ON ESP32

In order to perform the real-time processing and transmission of dynamic ECG signals and facilitate the upgrade of subsequent products, we select the ESP32-WROOM-32 of Le Xin Company as the main control chip. The chip's main advantage is low-power and has a Xtensa®32-bitLX6 single/dual-core processor, which has relatively strong computing power [38]. In addition, the chip also supports 2.4 GHZ Wi-Fi and Bluetooth protocols. The two functions can run at the same time and the data transmission has a good stability. The Bluetooth function can reach +12dBm

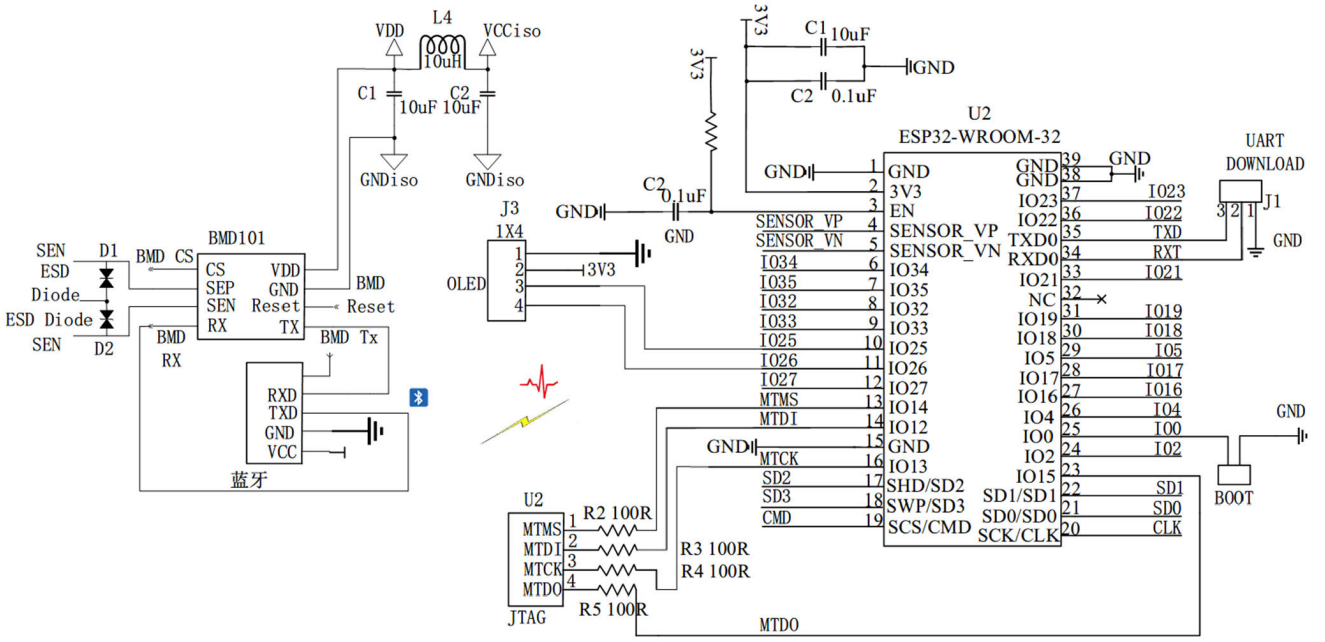

FIGURE 3. Main control unit circuit based on ESP32.

transmission power. The above performance can meet the requirements of data processing algorithm and transmission in this design. Figure 3 shows the schematic design of the main control unit based on the ESP32-WROOM-32 module. The wearable BMD101 module perform the data acquisition and Bluetooth transmission. The main control unit ESP32-WROOM-32 receives the patient's ECG signal through the built-in Bluetooth module. Then, it proceeds parsing, preprocessing and data compression, and it also utilizes the WIFI module of the module or the external 4G/5G module to upload the data to the cloud platform in real time. A 0.96 inch four-position OLED display is used to display the patient's heart rate and diagnosis results. In order to be portable, this design adopts a modular design, which integrates the ESP32-WROOM-32 module, OLED display screen and power module on a 28.5mm × 28mm PCB board.

IV. SOFTWARE PLATFORM

The wearable heart detector includes three modules: ECG acquisition, main control and cloud server. ECG acquisition module is mainly responsible for ECG signal acquisition, A/D conversion, data processing and transmission; ESP32 main control part is mainly responsible for data transmission with the cloud platform and acquisition block, ECG signal analysis, ECG waveform and diagnostic results analysis and display; The cloud server is mainly responsible for receiving and storing the ECG data sent by the main control, decompression, neural network diagnosis result, etc. Figure 4 shows the main working flow chart of the design, in which (a) is the overall process, (b) and (c) are the communication process between the acquisition module and the main control, the main control and the cloud platform respectively.

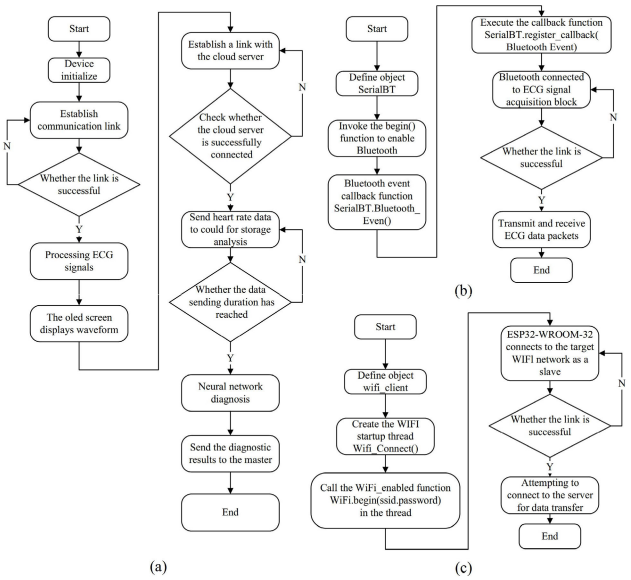

FIGURE 4. Working flow chart, (a) The overall process (b) The Bluetooth communication flow chart (c) the wifi communication flow chart.

ECG acquisition module adopts BMD101, which integrates the function of analog-to-digital conversion and ECG signal pre-processing. And band-pass filtering, median filtering and smooth filtering algorithms are used to preprocess the signal preliminary. The processed ECG data packet is sent to the main control unit through the Bluetooth module. The packet consists of three parts: data header, valid data to be sent, and check variable. Among them, the sampling rate is 512Hz, and the effective data is 16 bits.

The main control unit based on ESP32 module is responsible for the receiving, processing and remote transmission of the ECG signals. ESP32-WROOM-32 module resources include WI-FI module and Bluetooth module, wherein the Bluetooth communication module was started at the beginning of the program. However, the WIFI module is the thread which needs to be created after the successful startup of Bluetooth, and the two modules are synchronized after being enabled. Firstly, Call the library function BluetoothSerial.h to implement Bluetooth communication based on ESP32-WROOM-32 and write callback function SerialBT.Bluetooth_Even() to execute ECG data receiving, data parsing, etc., so that the Bluetooth module can always in the state of be started and working when the program is executed. Then, in the loop() function, the Bluetooth module is controlled for connection and normal data transmission according to whether it has successfully connected to the ECG signal acquisition module. At the same time, ESP32-WROOM-32 completes ECG data analysis and real-time waveform display. When the OLED display works, the start signal is first sent by the main control unit, and then the secondary address, read and write flag bits are sent. After the display is connected to the main control, 8 bits of data are transmitted to the main control each time, and the host replies to the reply signal after receiving it. When WI-FI is enabled on the ESP32, it is used as a secondary to connect to other WI-FI networks. By defining a WiFiClient class object wifi_client, create the thread function Wifi_Connect() which is started by the WI-Fi module to complete the start of WI-FI,and control whether the thread continues to connect to the WI-FI network to transmit data.

The remote cloud platform uses Alibaba Cloud server, it is based on ubuntu system to perform the data storge and multi-user SE-ResNet based lightweight arrhythmia recognition tasks. The network is gradually modified for different customers and the analysis results are returned to the client in time. ECG data acquisition and waveform display are shown in the figure 5.

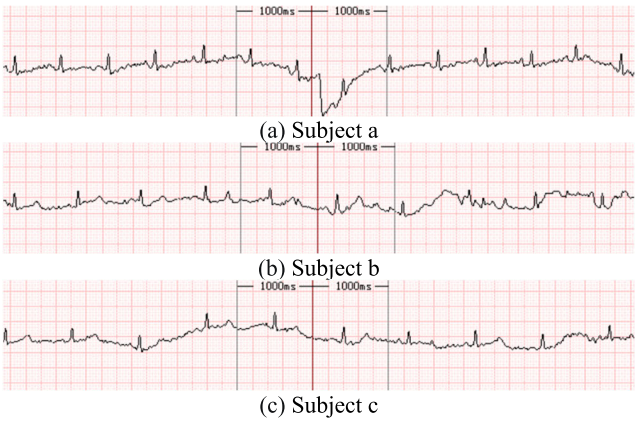

FIGURE 5. The Lead II ECG waveforms acquired from our device.

V. PVC REAL-TIME RECOGNITION AND IMPLEMENTATION BASED ON MULTI-PARAMETER SE-RESNET

A. DATA SOURCE AND PREPROCESSING

The experimental data were obtained from the MIT-BIH arrhythmia database and our acquisited data. The majority of lead-II ECGs from MIT-BIH arrhythmia database were used as training samples, the remainder and our device collected data are used to evaluate the proposed multi-parameter SE-ResNet model respectively. As the MIT-BIH database has a total of 48 records, each record is 30 minutes, and the sample rate is 360Hz. Each record consists of two leads. The lead of each record was not exactly the same, and only 46 records included MLII lead signals. The lead-II ECG from these 46 records were used in the following experiments, and all heartbeats are categorized into normal beats (N), premature ventricular beats (V), and other beats (T). Because the HRV parameter calculation needs to remove the first and last heartbeat of each record, a total of 105651 heartbeats were used for PVC recognition. Within this dataset, there are 74699, 8510, and 22442 N, V, and T heartbeats, respectively. 20000, 6500 and 10000 heartbeats were randomly selected from 74699 normal beats, 8510 ventricular premature beats and 22442 other beats respectively. A total of 36500 heartbeats were used as training samples. Similarly, 3000, 800 and 2000 cardiac beat data were randomly selected from the remaining N, V, and T heartbeats, respectively, and a total of 5800 data were used for evaluation, leaving the remaining 63,351 heartbeats for testing. To validate the reliability of the designed system and the proposed model, ECG data of 10 patients with ventricular premature disease and other arrhythmias were recorded using the wearable system. The acquisited ECG records were annotated by three clinical experts of the Fifth Affiliated Hospital of Zhengzhou University and a total of 6875 heartbeats were obtained. There are 4235,926,1714 for N, V and T, respectively.

The proposed approach's performance is gauged using accuracy (Acc), sensitivity (Se) and specificity (Sp). The specific calculation formula for each metric is as follows (1∼4):

$$Accuracy\,(A_{cc}) = \frac{TP + TN}{TP + TN + FP + FN} \tag{1}$$

$$Sensitivity\,(S_e) = \frac{TP}{TP + FN} \tag{2}$$

$$Specificity\,(S_p) = \frac{TN}{TN + FP} \tag{3}$$

$$Positive\ predictivity\,(P_p) = \frac{TP}{TP + FP} \tag{4}$$

All of the detection statistics are centered on the mutually exclusive categories of true positive (TP), false positive (FP), true negatives (TN), and false negative (FN) [39], [40], [41]. TP refers to accurate identification of a condition or trait while FP refers to incorrect identification of a condition or trait. TN refers to accurate identification of the absence of a

condition or trait whereas FN denotes incorrect identification of the absence of a condition or trait.

B. MULTI-PARAMETER SE-RESNET MODELING

Wearable ECGs exhibit individual variability and strong interference. Addressing these issues, our study adopts the SE-ResNet model, a deep network architecture with robust nonlinear fitting ability. The model incorporates a squeeze-excitation module embedded within a residual structure. The network model employs a feature recalculation strategy, automatically determining the importance of each feature channel by learning. Subsequently, useful features are enhanced, while the features not useful to the current task are suppressed based on their importance. Because the ECG has time-dependent features, such as double and triple rhythm, the characteristics such as heart rate variability (HRV) parameters and age, are important features for the arrhythmia recognition. As HRV parameters can compensate for the morphological characteristics of single heartbeat ECG. In this study, five characteristics: RR interval, ratio of RR interval before and after heartbeats, root mean square of the difference between adjacent RR intervals, age, and gender, are computed and integrated into the fully connected layer, providing useful information and effectively improving the model's classification accuracy.

In order to obtain the best network structure parameters and structures, SE-ResNet models with different layers and structures are designed, and repeated experiments and comparisons are made using MIT-BIH arrhythmia dataset. Figure 6 shows the cross-validation accuracy of MP-SE-ResNet networks with layers 8, 12, 16 and 20, respectively. As shown in the figure, the 16-layer SE-ResNet achieved better test results, and the performance of the 20-layer network was comparable to the 16-layer network. Considering the processing speed of wearable ECG data and the real-time requirements of the system, therefore, this paper chooses 16-layer SE-ResNet (Fig 6; Table 2) as the PVC recognition model.

As shown in Figure 7, the input single-channel ECG heartbeat size is 1×320, and after a layer of convolution, it is sent to the residual block, and 16,32 and 64 channels were selected respectively. The network model has 15 convolution layers and one fully connected layer in total. Take the first group of residual blocks (short-connect) as an example. In order to make better use of the context ECG characteristic information, channel level statistics are generated by global average pooling. The excitation layer adopts two fully connected layers (FC) to realize channel scaling, the reduction rate is set to 4, and the dimension of feature data is changed from 1×16 to 1×4, and then played back to 1×16. Finally, the activation function is used to re-scale the data back to the data dimensions before the squeeze. It is equivalent to mapping the data associated with the input to a set of channel weights, so that the channel features are not limited to the local receptive field of the convolutional network, and giving different weights to the channels.

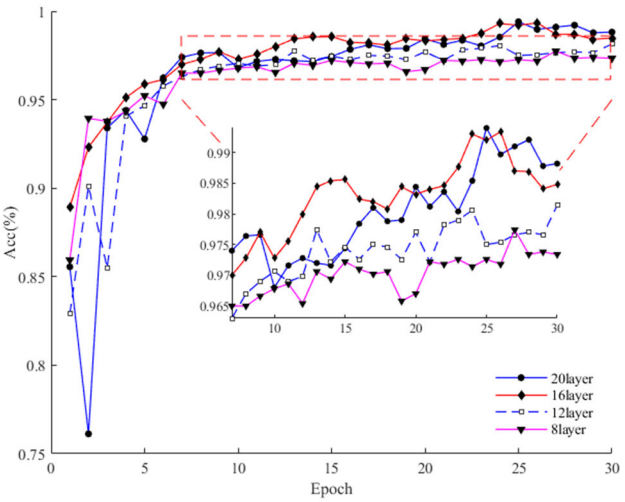

FIGURE 6. PVC recognition results of different network complexity.

TABLE 2. Details of the proposed SE-ResNet structure.

Layer Name	Input Size	Output Size	Operation
Conv1	1×230	1×59	Kernel Size:(1, 3), stride:2, padding:3 MaxPool: Kernel Size:3, stride:2, padding:1
Block1	1×59	1×59	$\begin{bmatrix}1\times3 & 16\\ 1\times3 & 16\end{bmatrix}\times2$
Block2	1×59	1×30	$\begin{bmatrix}1\times3 & 32\\ 1\times3 & 32\end{bmatrix}\times3$
Block3	1×30	1×15	$\begin{bmatrix}1\times3 & 64\\ 1\times3 & 64\end{bmatrix}\times2$
	1×15	1×15	BN, Relu,
	1×15		Flayer in Features:960, Output Features: NumClass

C. PVC RECOGNITION RESULTS BASED ON MP-SE-RESNET

In this work, the partial data of the MIT-BIH Lead-II ECG heartbeats are used for training the networks, the remaining and our device recorded data for evaluating the model, respectively. In order to avoid the chance of random data extraction, three random experiments were carried out, and the average value of the three experiments was taken as the final experimental result. The evaluation metrics derived from the experiments (Table 3) reveal that our proposed method achieves an overall recognition accuracy of 99.34% using the MIT-BIH database. The Se, Sp and Pp of PVC recognition reach 98.26%, 99.64%, and 84.03%, respectively. The overall recognition accuracy on our recorded data is 94.07%, with the Se, Sp and Pp yielding 92.76%, 97.63%, and 86.33%, respectively. Despite the imbalance in heartbeats within the MIT-BIH dataset, the experimental results underscore the effectiveness and robustness of the proposed model.

The ROC curves of the MIT-BIH and our recorded data are illustrated in Figure 8. Among them, Micro-average is a micro-average method which adds up the number of true positives, false positives and false negatives of all categories and then calculates the overall index. Macro-average is a

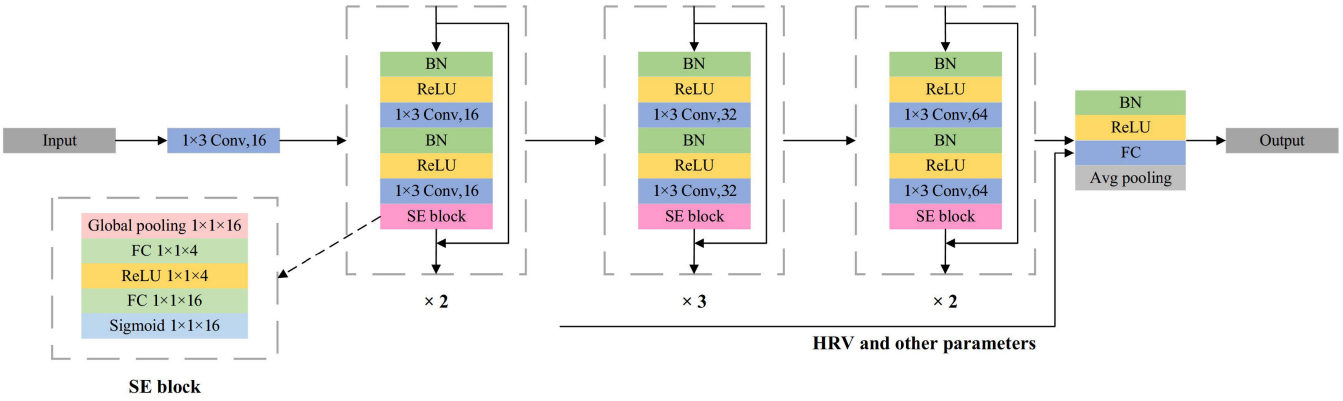

FIGURE 7. Deep MP-SE-ResNet learning network modeling.

macro average method, which calculates the metrics (such as sensitivity, positive and predictability) of each category and then uses the average of these metrics as the overall metric. Class 0, Class 1, and Class 2 represent N, V and T, respectively.

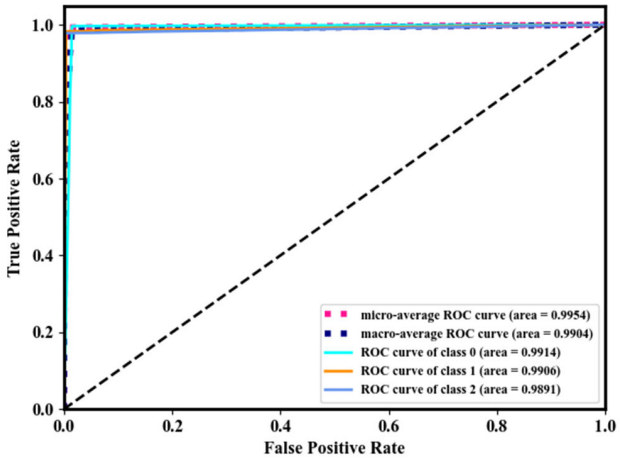

(a) MIT-BIH database

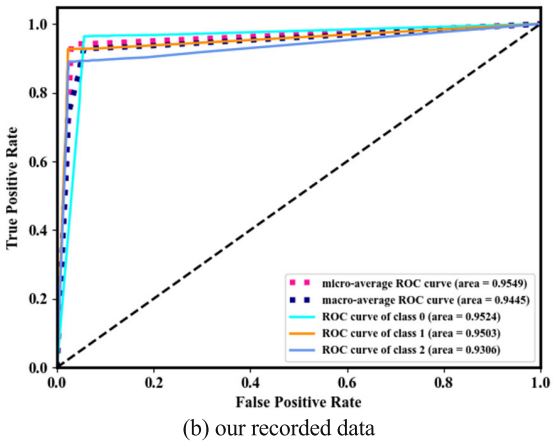

(b) our recorded data

FIGURE 8. ROC curves of using different database.

From Figure 8 (a) and (b), indicating that the model exhibits the best classification performance for the three type heartbeats. The area under the curve for N and V are the larger, the recognition result of the O type is relatively lower. The reason for being lower than N and V is that the sample size is too small.

TABLE 3. PVC recognition results based on MP-SE-ResNet.

Database		Confusion matrix			Evaluation metrics (%)			
		N	V	O	Se	Sp	Pp	Acc
MIT-BIH	N	51531	151	17	99.68	98.51	99.67	
	V	17	1189	4	98.26	99.64	84.03	99.34
	O	155	75	10212	97.8	99.96	99.79	
Our recorded	N	4083	49	103	96.41	94.15	96.5	
	V	46	859	21	92.76	97.63	86.33	94.07
	O	102	87	1525	88.97	97.55	92.48	

TABLE 4. Ablation experiment of MP-SE-ResNet.

Database	Modules			Acc(%)
	MP	SE	ResNet	
MIT-BIH			✓	97.43
		✓	✓	97.86
	✓		✓	97.82
	✓	✓	✓	99.34
Our recorded			✓	90.89
		✓	✓	92.53
	✓		✓	92.51
	✓	✓	✓	94.07

D. ABLIATION EXPERIMENTS AND COMPARISON OF DIFFERENT NETWORKS

To evaluate the effects of our proposed multi-parameter (MP) and squeeze-excitation (SE) block for the ResNet model. We performed experiments using the MP-SE-ResNET, MP-ResNet, SE-ResNet and ResNet respectively. The PVC recognition results on the MIT-BIH and our recorded databases of the five networks are depicted.

From Table 4, it can be observed that both the MP module and the SE module consistently improve the results, whether in the MIT-BIH dataset or in our recorded dataset. In the MIT-BIH dataset, the use of the SE module and ResNet module together results in a 0.43% improvement compared to using ResNet alone, while the use of the MP module and ResNet module together leads to a 0.39% improvement over using

ResNet alone. The combined use of the MP module and the SE module improves the results by 2.11% compared to not using these two modules. Similar improvements of 1.64%, 1.62%, and 3.18% are observed in our recorded dataset. Table 4 also indicates that the simultaneous use of the MP module and the SE module does not conflict; instead, their combined use yields greater improvement.

We compare our proposed approach with the published robust deep learning classifiers, such as ResNet, LSTM, CNN, and AlexNet. The same number of convolutional layers were designed, and the structural parameters were adjusted to the optimum. The same data were used to evaluate the networks respectively, and the results were compared. In the above experiments, the epoch is set to 30.

The PVC recognition results on the MIT-BIH and our recorded databases of the five networks mentioned before are depicted in Fig. 9 (a) and (b), respectively. As shown in Fig.9(a), SE-ResNet yields an improved overall accuracy of 1.52%, 1.68%, 3.46% and 7.25% compared to MP-ResNet, MP-LSTM, MP-CNN, and MP-AlexNet, respectively. In contrast, MP-SE-ResNet yields a Se of 98.26% for V, compared to 93.88%, 92.64%, 83.97% and 81.4% of MP-ResNet, MP-LSTM, MP-CNN, and MP-AlexNet, respectively. The overall recognition accuracy of our designed MP-SE-ResNet is 99.34%. The proposed model outperforms other existing models. Using our recorded data, the proposed MP-SE-ResNet model yields higher overall accuracy and enhanced accuracy and sensitivity of PVC recognition in abnormal heartbeat detection tasks. The accuracy of the developed SE-ResNet algorithm is 94.07%, higher than MP-ResNet, MP-LSTM, MP-CNN, and MP-AlexNet. The Se of premature ventricular contractions recognition is 92.76%, compared to 86.61%, 85.96%, 79.16% and 84.77% of MP-ResNet, MP-LSTM, MP-CNN and MP-AlexNet, respectively. It can be seen from the figure that the model used in this paper has better results than other models. Moreover, the 16-layer network has low complexity, high efficiency and convenient real-time implementation, so it has certain application value.

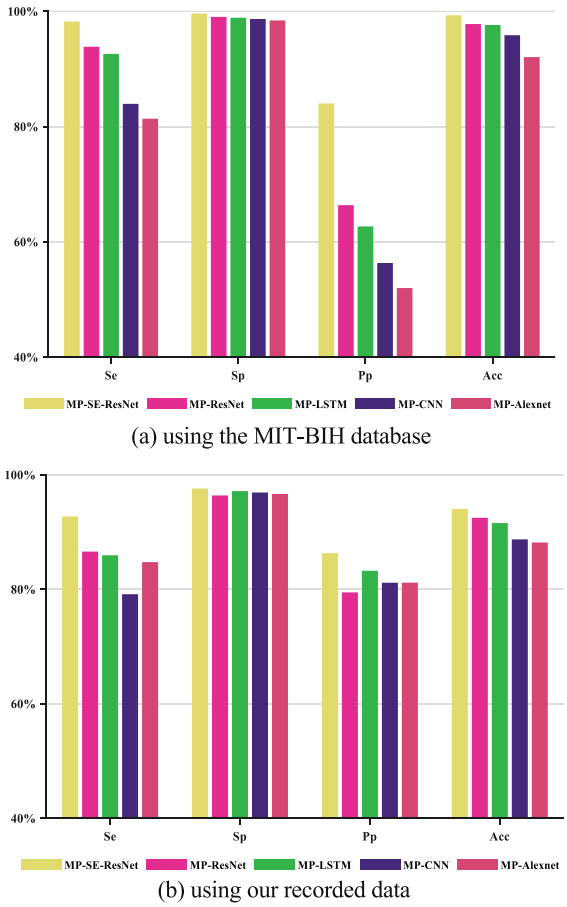

FIGURE 9. Results of PVC recognition of using different classifiers.

VI. DISCUSSION

ECG is the gold standard for arrhythmias detection. Development of wearable and Internet of Things (IoT) technologies enables the real-time and continuous individual ECG monitoring and arrhythmia diagnosis. The existing key technology challenges are mainly including the hardware implementation, the real-time signal analysis performed on the embedded processor and the cloud computing for long-term ECG disease type mining. In this paper, we designed a wearable dynamic single lead ECG SmartVest system based on the MP-SE-ResNet model. We proposed the system hardware and software design in detail, and also the ECG preprocessing real-time PVC recognition system are developed and the experiments are performed.

As wearable dynamic ECG exhibits strong background noise and variability. Furthermore, ECG is weak time domain waveform, and the microvariation of its morphological characteristics is key for arrhythmia recognition. But the microvariation of the ECG waveform is easily arise the gradient disappearance of the deep-CNN networks. The residual network aims to solve the gradient disappearance issue in deep neural networks by incorporating a residual block. This mechanism allows the network to adapt to the network structure of any depth by learning the residual. The squeeze-excitation network incorporates the attention mechanism, automatically determining the importance of each feature channel through learning. This mechanism promotes useful features and suppresses less useful features following their importance. The network model comprehensively considers the weight of each channel and the main wave of ECG signals. Therefore, it can fully extract the morphological features from multiple channels and their primary waves, enhancing the network's robustness and generalization capability.

The heartbeats are categorized into classes, and the confusion matrix on the MIT-BIH and our recorded databases are depicted in Figs. 10 and 11, respectively. The proposed MP-SE-ResNet network demonstrates excellent performance in PVC recognition experiments using single-lead long-term ECGs. However, the network produces suboptimal recognition results of the third class in the MIT-BIH database

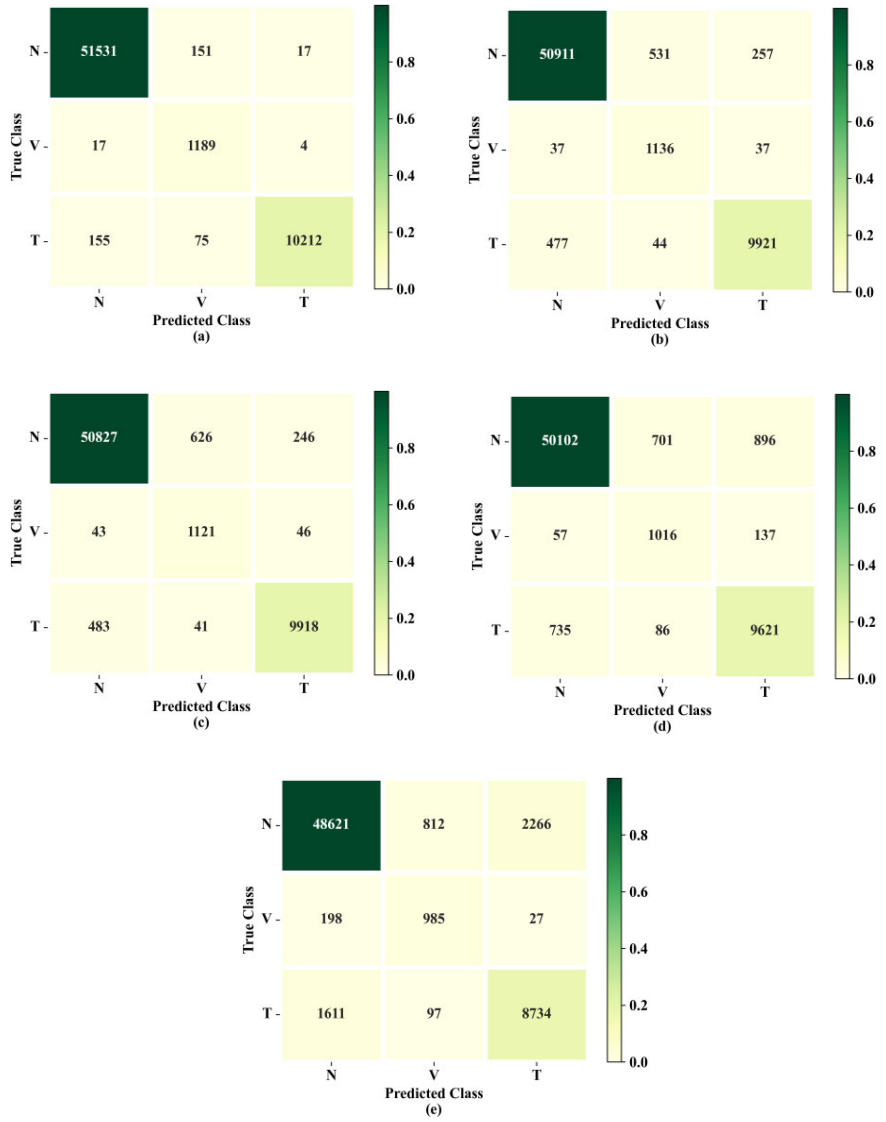

FIGURE 10. Confusion matrix of different networks on the MIT-BIH database. (a) MP-SE-ResNet; (b) MP-ResNet; (c) MP-LSTM; (d) MP-CNN; (e) MP-AlexNet.

due to data imbalance, with an excessive amount of the first type and a limited number of other types.

We investigated the open-access published PVC recognition literature on the MIT-BIH database (Table 5). Acharya et al. [42] developed a deep convolutional network model to classify heartbeats. The MIT-BIH database is employed for classification, and the model yields an overall classification accuracy and Se of 94.03% and 94.07%, respectively. Wang et al. [43] proposed an ECG technique based on multi-lead signals and a deep learning architecture. Automatic identification of ECG signals is performed using the INCART arrhythmia database, producing an overall classification accuracy and Se of 93.40% and 84.10%, respectively. Niu et al. [44] employed three morphological and seven statistical features and developed an artificial neural network (ANN) classifier for PVC and non-PVC ECG heartbeat recognition. The classification accuracy and Se of PVC achieved using the MIT-BIH dataset are 96.40% and 85.70%, respectively. Wang [29] proposed an improved gated recurrent unit (IGRU) by setting a scale parameter into existing bidirectional GRU (BGRU) model for PVC signals recognition. The experimental results of the model on the MIT-BIH database yields the recognition accuracy of 98.3%. Sarshar and Mirzaei [30] explored a combined statistical features and CNN model for PVC recognition on the MIT-BIH database, producing more effective diagnosis performance. Cai et al. [24] developed a novel PVC recognition algorithm that combined deep learning-based heartbeat template cluster and expert system-based heartbeat classifier. The PVC identification Se, P+ and ACC are 87.51%, 92.47% and 98.63%, respectively. Harkat and Benzid [45] proposed a DCT and CWT feature extraction and RBF classifier for PVC

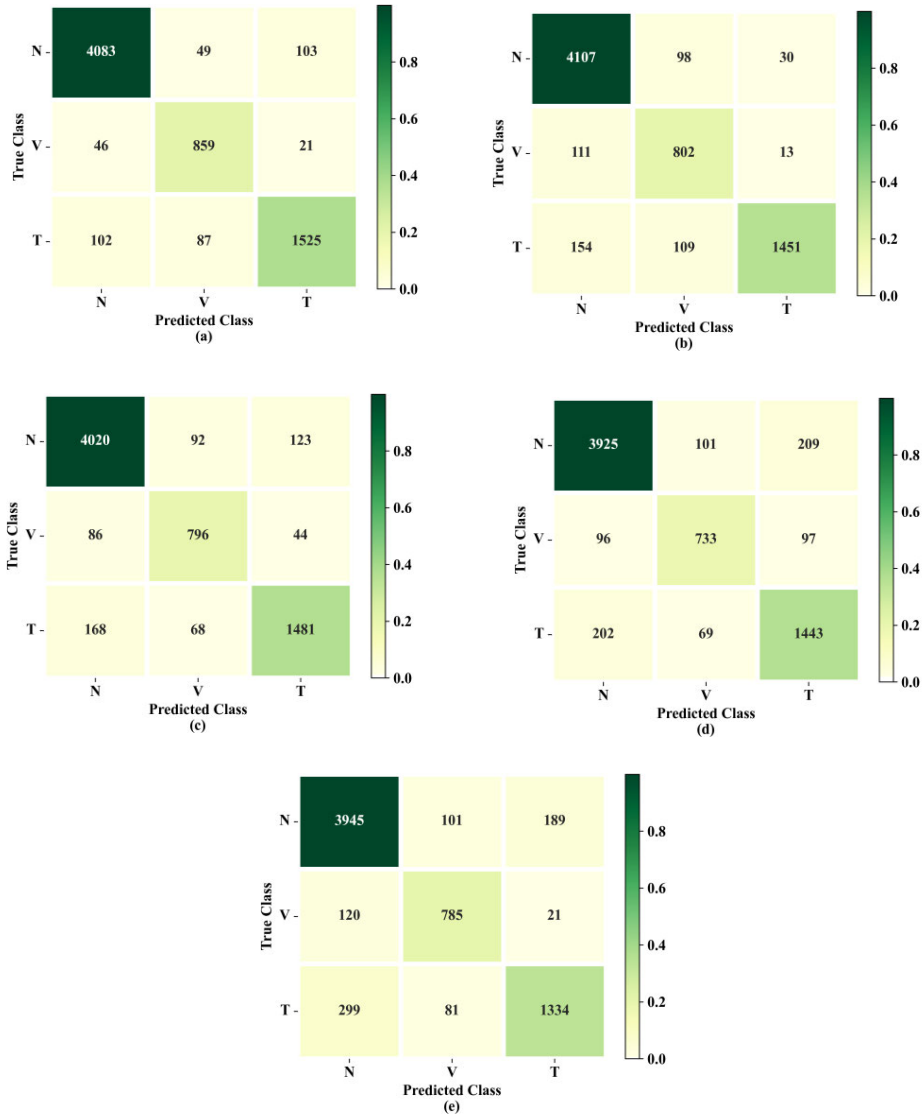

FIGURE 11. Confusion matrix of different networks on our recorded database. (a) MP-SE-ResNet; (b) MP-ResNet; (c) MP-LSTM; (d) MP-CNN; (e) MP-AlexNet.

TABLE 5. Comparison of PVC recognition results.

Method	Year	Number of classes	Se	Acc
Acharya et al. [42]	2017	5	94.07%	94.03%
Wang et al. [43]	2020	3	84.10%	93.40%
Niu et al. [44]	2020	3	85.70%	96.40%
Wang et al. [29]	2021	2	97.9%	98.3%
Sarshar et al. [30]	2022	2	99.2%(N+V)	*
Cai et al. [24]	2022	2	87.51%	98.63%
Harkat et al. [45]	2023	2	95.2%	98.2%
Algorithm in this paper	2024	3	98.26%	99.34%

TABLE 6. Comparison of Computational Complexity with similar method.

Method	Year	layers	Maximum kernel size	MParams	MFLOPs	Acc(%)
Acharya et al. [42]	2017	6	(1,4)	127335	1.206	94.03
Wang et al. [43]	2020	9	128	65060	0.129	93.40
Niu et al. [44]	2020	7	(1,30)	360448	3.978	96.40
Algorithm in this paper	2024	16	(1,3)	23791	3.739	99.34

recognition, achieving an overall sensitivity of 95.2% and an accuracy of 98.2%. The discussed literature highlights the superior sensitivity of the proposed SE-ResNet in recognizing PVCs in wearable ECG, which is of clinical significance.

To evaluate the algorithm complexity, of our method, we compared our method with the recently published algorithms in Table 6. Where Params represents the number

of parameters in the entire network; MFLOPs stands for Million Floating Point Operations Per Second, indicating the computational complexity of the model; Maximum kernel size refers to the largest one-dimensional convolutional kernel size or the number of units in the fully connected (FC) layer. In the proposed MP-SE-ResNet in this paper, the network primarily utilizes convolutional and fully connected layers to extract and transform features from input data. Therefore, similar algorithms were selected for comparison of network complexity. In previous studies, most networks chose shallow networks (less than 10 layers) for classification. Due to the shallow network depth, larger-sized (or quantity) convolutional kernels or more units in the fully connected layers were needed to extract sufficiently discriminative features, resulting in a large number of parameters. The method used in this paper achieves higher classification accuracy by stacking multiple convolutional kernels of small sizes and multiple FC layers with a small number of units. However, inevitably, better performance may lead to higher computational costs. We noticed that methods using CNNs (except for Arivarasi et al. [36], who used two parallel multilayer FC layers) generally result in higher computational complexity, consistent with the principles of deep learning, as convolutional operations are more complex than matrix multiplication. Compared to other methods, MP-SE-ResNet achieves a balance in performance, number of parameters, and model computational complexity.

VII. CONCLUSION

This paper proposes a design scheme of a multi-scene wearable wireless ECG acquisition and real-time auxiliary analysis system, and completes the software and hardware design and algorithm effect test. Based on multi-parameter deep SE-ResNet network, the recognition of single lead wearable ECG signal ventricular premature beat was realized. BMD101 ECG acquisition module and ESP32 primary control unit to complete real-time acquisition and ECG preprocessing. We also developed a real-time PVC recognition software based on multi-parameter SE-ResNet model. MIT-BIH lead-II ECG arrhythmia data were used as training samples. The whole recognition accuracy on the remaining MIT-BIH arrhythmia dataset was 99.34%, and the Se and Sp were 98.26% and 98.94% respectively. The recognition accuracy of our recorded data was 92.54%, and the Se and Sp of V reached 91.68% and 97.60%, respectively. Experimental results demonstrated that our proposed model outperforms other existing models. The system is economical and reliable, and provides technical ideas for chronic cardiac disease management and real-time monitoring of arrhythmia, and has certain popularization and application value. Considering the real-time operation of the ECG monitoring and the non-balance of Arrhythmia data, in the future research, we will focus on the highly efficient ECG data compression algorithm and the exploring of robust classification strategies for handling imbalanced ECG data.

REFERENCES

[1] A. Odutayo, C. X. Wong, A. J. Hsiao, S. Hopewell, D. G. Altman, and C. A. Emdin, "Atrial fibrillation and risks of cardiovascular disease, renal disease, and death: Systematic review and meta-analysis," *BMJ*, vol. 354, p. 4482, Sep. 2016.

[2] J. Kingma, C. Simard, and B. Drolet, "Overview of cardiac arrhythmias and treatment strategies," *Pharmaceuticals*, vol. 16, no. 6, p. 844, Jun. 2023.

[3] A. Alloubani, R. Nimer, and R. Samara, "Relationship between hyperlipidemia, cardiovascular disease and stroke: A systematic review," *Current Cardiol. Rev.*, vol. 17, no. 6, 2021, Art. no. e051121189015.

[4] Y. Li, Z. Zhang, F. Zhou, Y. Xing, J. Li, and C. Liu, "Multi-label classification of arrhythmia for long-term electrocardiogram signals with feature learning," *IEEE Trans. Instrum. Meas.*, vol. 70, pp. 1–11, 2021.

[5] M. Dai, X. Xiao, X. Chen, H. Lin, W. Wu, and S. Chen, "A low-power and miniaturized electrocardiograph data collection system with smart textile electrodes for monitoring of cardiac function," *Australas. Phys. Eng. Sci. Med.*, vol. 39, no. 4, pp. 1029–1040, Dec. 2016.

[6] C. Liu, M. Yang, J. Di, Y. Xing, Y. Li, and J. Li, "Wearable ECG: History, key technologies and future challenges," *Chin. J. Biomed. Eng.*, vol. 38, no. 6, pp. 641–652, 2019.

[7] J. Hayano and E. Yuda, "Assessment of autonomic function by long-term heart rate variability: Beyond the classical framework of LF and HF measurements," *J. Physiolog. Anthropol.*, vol. 40, no. 1, p. 21, Nov. 2021.

[8] C. Liu, X. Zhang, L. Zhao, F. Liu, X. Chen, Y. Yao, and J. Li, "Signal quality assessment and lightweight QRS detection for wearable ECG SmartVest system," *IEEE Internet Things J.*, vol. 6, no. 2, pp. 1363–1374, Apr. 2019.

[9] A. John, S. J. Redmond, B. Cardiff, and D. John, "A multimodal data fusion technique for heartbeat detection in wearable IoT sensors," *IEEE Internet Things J.*, vol. 9, no. 3, pp. 2071–2082, Feb. 2022.

[10] J. R. Windmiller and J. Wang, "Wearable electrochemical sensors and biosensors: A review," *Electroanalysis*, vol. 25, no. 1, pp. 29–46, Jan. 2013.

[11] M. T. I. U. Huque, K. S. Munasinghe, and A. Jamalipour, "Body node coordinator placement algorithms for wireless body area networks," *IEEE Internet Things J.*, vol. 2, no. 1, pp. 94–102, Feb. 2015.

[12] Z. Cai, K. Luo, C. Liu, and J. Li, "Design of a smart ECG garment based on conductive textile electrode and flexible printed circuit board," *Technol. Health Care*, vol. 25, no. 4, pp. 815–821, Aug. 2017.

[13] S. Izumi, K. Yamashita, M. Nakano, H. Kawaguchi, H. Kimura, K. Marumoto, T. Fuchikami, Y. Fujimori, H. Nakajima, T. Shiga, and M. Yoshimoto, "A wearable healthcare system with a 13.7 μ a noise tolerant ECG processor," *IEEE Trans. Biomed. Circuits Syst.*, vol. 9, no. 5, pp. 733–742, Oct. 2015.

[14] S. Amendola, R. Lodato, S. Manzari, C. Occhiuzzi, and G. Marrocco, "RFID technology for IoT-based personal healthcare in smart spaces," *IEEE Internet Things J.*, vol. 1, no. 2, pp. 144–152, Apr. 2014.

[15] Z. Li, D. Zhou, L. Wan, J. Li, and W. Mou, "Heartbeat classification using deep residual convolutional neural network from 2-lead electrocardiogram," *J. Electrocardiol.*, vol. 58, pp. 105–112, Jan. 2020.

[16] S. Saadatnejad, M. Oveisi, and M. Hashemi, "LSTM-based ECG classification for continuous monitoring on personal wearable devices," *IEEE J. Biomed. Health Informat.*, vol. 24, no. 2, pp. 515–523, Feb. 2020.

[17] V. Avula, K. C. Wu, and R. T. Carrick, "Clinical applications, methodology, and scientific reporting of electrocardiogram deep-learning models," *JACC, Adv.*, vol. 2, no. 10, Dec. 2023, Art. no. 100686.

[18] N. Farzaneh, H. Ghanbari, M. Liu, L. Cao, K. R. Ward, and S. Ansari, "A comprehensive comparison of six publicly available algorithms for localization of QRS complex on electrocardiograph," in *Proc. 45th Annu. Int. Conf. IEEE Eng. Med. Biol. Soc. (EMBC)*, Jul. 2023, pp. 1–4.

[19] H. Moroz, Y. Li, and A. Marelli, "HART: Deep learning-informed lifespan heart failure risk trajectories," *Int. J. Med. Informat.*, vol. 185, May 2024, Art. no. 105384.

[20] W.-W. Chen, C.-C. Tseng, C.-C. Huang, and H. H.-S. Lu, "Improving deep-learning electrocardiogram classification with an effective coloring method," *Artif. Intell. Med.*, vol. 149, Mar. 2024, Art. no. 102809.

[21] T. Tuncer, S. Dogan, P. Pławiak, and U. R. Acharya, "Automated arrhythmia detection using novel hexadecimal local pattern and multilevel wavelet transform with ECG signals," *Knowl.-Based Syst.*, vol. 186, Dec. 2019, Art. no. 104923.

[22] D. Li, R. Shi, N. Yao, F. Zhu, and K. Wang, "Real-time patient-specific ECG arrhythmia detection by quantum genetic algorithm of least squares twin SVM," *J. Beijing Inst. Technol.*, vol. 29, no. 1, pp. 29–37, 2020.
[23] J. Linpeng and D. Jun, "Deep learning algorithm for clinical ECG analysis," *Sci. China, Inf. Sci.*, vol. 45, no. 3, pp. 398–416, 2015.
[24] Z. Cai, T. Wang, Y. Shen, Y. Xing, R. Yan, J. Li, and C. Liu, "Robust PVC identification by fusing expert system and deep learning," *Biosensors*, vol. 12, no. 4, p. 185, Mar. 2022.
[25] H. Ullah, M. B. B. Heyat, F. Akhtar, A. Y. Muaad, C. C. Ukwuoma, M. Bilal, M. H. Miraz, M. A. S. Bhuiyan, K. Wu, R. Damaševičius, T. Pan, M. Gao, Y. Lin, and D. Lai, "An automatic premature ventricular contraction recognition system based on imbalanced dataset and pre-trained residual network using transfer learning on ECG signal," *Diagnostics*, vol. 13, no. 1, p. 87, Dec. 2022.
[26] G. Petmezas, K. Haris, L. Stefanopoulos, V. Kilintzis, A. Tzavelis, J. A. Rogers, A. K. Katsaggelos, and N. Maglaveras, "Automated atrial fibrillation detection using a hybrid CNN-LSTM network on imbalanced ECG datasets," *Biomed. Signal Process. Control*, vol. 63, Jan. 2021, Art. no. 102194.
[27] B. Hou, J. Yang, P. Wang, and R. Yan, "LSTM-based auto-encoder model for ECG arrhythmias classification," *IEEE Trans. Instrum. Meas.*, vol. 69, no. 4, pp. 1232–1240, Apr. 2020.
[28] C. Brito, A. Machado, and A. Sousa, *Electrocardiogram Beat-Classification Based on a ResNet Network* (Studies in Health Technology and Informatics), vol. 264. 2019, pp. 55–59.
[29] J. Wang, "Automated detection of premature ventricular contraction based on the improved gated recurrent unit network," *Comput. Methods Programs Biomed.*, vol. 208, Sep. 2021, Art. no. 106284.
[30] N. T. Sarshar and M. Mirzaei, "Premature ventricular contraction recognition based on a deep learning approach," *J. Healthcare Eng.*, vol. 2022, pp. 1–7, Mar. 2022.
[31] M. Ebrahimpoor, M. Taghizadeh, M. H. Fatehi, O. Mahdiyar, and J. Jamali, "Premature ventricular contractions detection by multi-domain feature extraction and auto-encoder-based feature reduction," *Circuits, Syst., Signal Process.*, vol. 43, no. 5, pp. 3279–3296, May 2024.
[32] A. Gon and A. Mukherjee, "Design of hardware-efficient PVC recognition and classification system for early detection of sudden cardiac arrests," *AEU-Int. J. Electron. Commun.*, vol. 172, Dec. 2023, Art. no. 154955.
[33] I. Silva, G. B. Moody, and L. Celi, "Improving the quality of ECGs collected using mobile phones: The PhysioNet/computing in cardiology challenge 2011," in *Proc. Comput. Cardiol.*, Sep. 2011, pp. 273–276.
[34] S. Hong, Y. Zhou, J. Shang, C. Xiao, and J. Sun, "Opportunities and challenges of deep learning methods for electrocardiogram data: A systematic review," *Comput. Biol. Med.*, vol. 122, Jul. 2020, Art. no. 103801.
[35] S. Kaptoge et al., "World Health Organization cardiovascular disease risk charts: Revised models to estimate risk in 21 global regions," *Lancet Global Health*, vol. 7, pp. e1332–e1345, 2019.
[36] A. Arivarasi, D. Thiripurasundari, A. A. Selvakumar, B. Kumaar, T. Aghil, S. Rahul, and R. Kannan, "An advanced cost-efficient IoT method for stroke rehabilitation using smart gloves," *Nanotechnol. Precis. Eng.*, vol. 6, no. 4, pp. 1–15, Dec. 2023.
[37] Y.-L. Zheng, X.-R. Ding, C. C. Y. Poon, B. P. L. Lo, H. Zhang, X.-L. Zhou, G.-Z. Yang, N. Zhao, and Y.-T. Zhang, "Unobtrusive sensing and wearable devices for health informatics," *IEEE Trans. Biomed. Eng.*, vol. 61, no. 5, pp. 1538–1554, May 2014.
[38] S. A. Siddiqui, Y. Zhang, Z. Feng, and A. Kos, "A pulse rate estimation algorithm using PPG and smartphone camera," *J. Med. Syst.*, vol. 40, no. 5, pp. 1–6, May 2016.
[39] P. Liu, X. Sun, Y. Han, Z. He, W. Zhang, and C. Wu, "Arrhythmia classification of LSTM autoencoder based on time series anomaly detection," *Biomed. Signal Process. Control*, vol. 71, Jan. 2022, Art. no. 103228.
[40] W. Zeng and C. Yuan, "ECG arrhythmia classification based on variational mode decomposition, Shannon energy envelope and deterministic learning," *Int. J. Mach. Learn. Cybern.*, vol. 12, no. 10, pp. 2963–2988, Oct. 2021.
[41] P. M. Tripathi, A. Kumar, R. Komaragiri, and M. Kumar, "A review on computational methods for denoising and detecting ECG signals to detect cardiovascular diseases," *Arch. Comput. Methods Eng.*, vol. 29, no. 3, pp. 1875–1914, May 2022.
[42] U. R. Acharya, S. L. Oh, Y. Hagiwara, J. H. Tan, M. Adam, A. Gertych, and R. S. Tan, "A deep convolutional neural network model to classify heartbeats," *Comput. Biol. Med.*, vol. 89, pp. 389–396, Oct. 2017.
[43] H. Wang, H. Shi, K. Lin, C. Qin, L. Zhao, Y. Huang, and C. Liu, "A high-precision arrhythmia classification method based on dual fully connected neural network," *Biomed. Signal Process. Control*, vol. 58, Apr. 2020, Art. no. 101874.
[44] J. Niu, Y. Tang, Z. Sun, and W. Zhang, "Inter-patient ECG classification with symbolic representations and multi-perspective convolutional neural networks," *IEEE J. Biomed. Health Informat.*, vol. 24, no. 5, pp. 1321–1332, May 2020.
[45] A. Harkat and R. Benzid, "Premature ventricular contraction (PVC) recognition using DCT-CWT based discriminant and optimized RBF neural network," *J. Biomimetics, Biomater. Biomed. Eng.*, vol. 60, pp. 109–117, May 2023.

DUAN LI was born in 1979. She received the Ph.D. degree. She is currently an Associate Professor. Her research interests include biological signal processing and machine learning.

PEISEN LIU was born in 1998. He is currently pursuing the degree with Zhengzhou University of Light Industry. His research interests include brain–computer interface signal processing and recognition.

TINGTING SUN was born in 1998. She is currently pursuing the master's degree. Her research interest includes machine learning.

LIANXIANG LI was born in 2000. He is currently pursuing the degree with Zhengzhou University of Light Industry. His research interests include brain–computer interface and embedded system design.

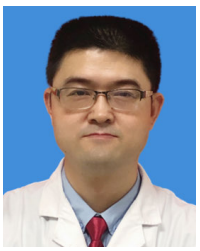

YIBAI XUE was born in 1978. He received the master's degree. He is currently the Chief Physician. His research interests include cardiac electrophysiology and minimally invasive surgery.